Human red blood cell aging:
correlative changes in surface charge and cell properties

Yao-Xiong Huang [a, *], Zheng-Jie Wu [a], Jitendra Mehrishi [b, c], Bao-Tian Huang [a],
Xing-Yao Chen [a], Xin-Jing Zheng [a], Wen-Jing Liu [a], Man Luo [a]

[a] *Institute of Biomedical Engineering, Ji Nan University, Guang Zhou, China*
[b] *University of Cambridge, Cambridge, UK*
[c] *The Cambridge Blood, Stem, Sperm Cells, Doping and High Altitude Research Initiative, Impington, Cambridge, UK*

Abstract

Red blood cells (RBCs) during microcirculation, aging and storage, lose *N*-acetylneuraminic acid (NANA) and other biomaterials thereby altering cell structures, some properties and functions. Such cell damage very likely underlies the serious adverse effects of blood transfusion. However, a controversy has remained since 1961–1977 as to whether with aging, the RBCs, suffering loss of NANA, do have a decreased charge density. Any correlation between the changes in the cell properties with cell aging is also not clear. Therefore, to remove the ambiguity and uncertainty, we carried out multiparameteric studies on Percoll fractions of blood of 38 volunteers (lightest-young-Y-RBCs, densest-old-O-RBCs, two middle fractions).We found that there were striking differences between the properties of Y-RBCs and O-RBCs. The ζ-potential of Y-RBCs decreased gradually with aging. Studies in parallel on RBC fractions incubated with both positively charged quantum dots and *Sambucus Nigra*-fluorescein isothiocyanate (FITC) along with their ζ-potentials provide for the first time direct visual evidence about the lesser amount of charge density and NANA on O-RBCs, and a collinear decrease in their respective ζ-potentials. Close correlation was found between the surface charge on an aging RBC and its structure and functions, from the cell morphology, the membrane deformability to the intracellular Hb structure and oxidation ability. This quantitative approach not only clarifies the picture but also has implications in biology and medicine.

Keywords: red blood cell • RBC aging and storage • surface charge • structure and functions • haemoglobin

Introduction

Red blood cell (RBC) aging in health, disease and storage is of considerable interest. During aging/storage, RBCs lose water, 2,3-bisphosphoglyceric acid, ATP, proteins, Hb and vesicles leading to decreasing cell volume, surface charge and increasing density. There is also a decrease of pH and generation of cytokines and bioreactive substances in preserved blood [1–7].

Circulating RBCs are of biconcave discoid shape, 7.8×1.8 μm, 1 μm thin in the middle. They possess unique deformability, thus being able to squeeze through capillaries as narrow as 1.8 μm. During the ~240 km journey in their life span (~120 days), they incessantly squeeze through narrow capillaries [1–3]. As RBCs become aged, some surface materials, *e.g.* sialoglycoproteins-sialic acids (SA), get sheared off and RBC structures/properties change. *In vivo*, aging RBCs [8, 9] undergo membrane changes in band-3 (the erythrocyte anion exchanger) and the neoantigens that appear bind autologous immunoglobulin-G [8], such aged cells become targets for grabbing by macrophages in the spleen (liver, bone marrow) for elimination by the reticuloendothelial system (RES). The biomaterials discharged [1–3] from stored RBCs affecting cell properties are thought to cause serious side effects of transfusing blood that is older than 14 days [3, 10–12]. In severe trauma patients, transfusion of blood stored for more than 28 days doubled the incidence of deep vein thrombosis and increased death secondary to multiple organ failure [11].

Mammalian cells are covered by glycoconjugates. RBCs, RBC stroma treated with *V.cl.*-derived receptor destroying enzyme-(neuraminidase, lyophilized) released SAs [13–15]. Human RBC-SAs were found to contain 95% *N*-acetylneuraminic acid (NANA). Piper [16] was the first to report that RBCs treatment with this

*Correspondence to: Yao-Xiong HUANG,
Institute of Biomedical Engineering,
Ji Nan University, Guang Zhou 510632, China.
Tel.: 86–20-85220469
Fax: 86–20-85223742
E-mail: tyxhuang@jnu.edu.cn

enzyme decreased their electrophoretic mobility (EPM) by ~80%. Klenk proposed [14] that α-carboxyls of RBC-NANA generated RBC electrical charge determined by cell electrophoresis [17–19]. Four years later, others [20, 21] confirmed a 74–94% decrease of RBC-EPMs with a concomitant release of NANA.

Decreased EPM of RBCs, *e.g.* by neuraminidase, implies cells carrying decreased numbers of NANA-carboxyls [18–21]. Decreased EPM of RBCs also implies cells carrying lesser charge density (σ) and ζ-potential, which can be derived using the Smoluchowski equation [17–19].

There is a significant biological relevance of RBC surface SA [22], remaining intact for membrane structure, shape, function and RBC survival [23]. One of the major physico-chemical factors that governs cell interactions is the electrical charge arising from NANA carboxyls and other ionizable chemical groups [17–19], which thus have a biological relevance [24]. ζ-potential, which was measured without subjecting cells to unduly harsh treatment, is recognized as a useful probe for information and monitoring membrane events/changes on live/intact cells [17–19].

Using phthalate esters Danon and Marikowsky [24] fractionated blood into the lightest and the densest RBCs and found EPMs of the densest RBCs decreased by ~23% (10 donors-Israeli). Fractionated cells before and after neuraminidase treatment labelled with colloidal iron particles [25] showed diminished charge density (EPM) on senescent-RBCs, attributable to partially lost membrane-bound-NANA charge. Yaari [26] confirmed 31–41% decreased EPMs of O-RBCs (11 donors-Israeli). Two studies [27, 28] on the blood of six US–Caucasian donors each, fractionated by density alone or phthalate esters, did not confirm decreased EPMs of O-RBCs. However, neuraminidase treatment consistently released [27, 28] 12% lesser amount of NANA from O-RBCs. The inconclusive data on 30–40 cells each from just 3 to 6–11 donors perhaps resulted from different methods; lighter cells were lost during washing-technical difficulties and limitations of the manual instrument that after all was designed in the 1920s.

Apart from the controversy about the decrease of surface charge of aging RBCs, it was of great importance to discover whether there were any changes in the other properties of RBCs with aging, such as the structure of intracellular Hb and oxygenation ability. Any correlation between the changes in the properties with cell aging has not been clear.

In view of the recently increased importance of RBC aging *in vivo*/plastic bags and blood storage damage [1–3, 10–12], it is necessary to confirm whether cell aging would lead to a decrease of the surface SA and surface charge/ζ-potential, thereby inducing a series of changes in cell properties, including the cell morphology, membrane flexibility and the structure of intracellular Hb, as well as its oxygenation ability.

Therefore, to discover the causes for the underlying differences between the data obtained by three groups of workers during 1961–1977, we carried out multiparameteric systematic detailed studies in parallel on aliquots of RBC fractions harvested from the blood of 38 non-smoking adults (23–26 years of age) (24 men; 14 women, 2 who were 35 years old, none of whom taking contraceptive pills). Fractionation of blood was performed by both Percoll and high-speed centrifugation to find out if the method of fractionation would yield satisfactory comparable or different results. RBC fractions obtained were the lightest/young-RBCs (Y), the densest/old RBCs (O) and two middle fractions (M1, M2). All the fractions were used for investigations of ζ-potentials; fluorescence from cell-bound SA-specific lectin FITC *Sambucus Nigra* (*SNA*-FITC) for the amount/density of SA; fluorescence intensity from cell-bound quantum dots (QDs, positively charged that label all the electron charges) for quantitative visualization of all the surface charges; membrane bending modulus (K_c) and the ability of the cells getting through capillary which reflects the membrane deformability; cell morphology and the Raman microscopy of intracellular Hb in intact RBCs.

Materials and methods

Studies on blood of volunteers (providing informed written consent) were approved by Ji Nan University Animal Care and Use Committee conforming to the Chinese Public Health Service Policy on Human Care and Use of Laboratory Animals.

Venous blood of 38 non-smoking healthy 23–26-year-old adult volunteers (Guangzhou, China, mostly laboratory personnel, providing informed written consent, 24 men, 14 women, 2 married women 35 years of age, none taking contraceptive pill) was investigated. Blood, drawn by venepuncture (usually, at ~9 a.m.) collected into heparin-containing tubes was centrifuged (2000 $\times$ *g*; 10 min., 4°C), plasma and buffy coat removed and cells washed three times with isotonic phosphate-buffered saline (90 mM NaCl, 50 mM sodium phosphate, 5 mM KCl, 6 mM glucose, pH 7.4, ionic strength 0.029).

RBC fractionation

Percoll fractionation: Blood (diluted with buffer 1:1) was centrifuged (2700 $\times$ *g*, 20 min., 4°C) over Percoll gradients (densities varying from 1.065-1.080 g/ml or 1.075-1.115 g/ml). This provided four fractions: the lightest/top/young-Y-RBCs, the densest-old-O-RBCs, middle fractions, M1 and M2. Harvested cells washed with isotonic buffer were suspended in 0.029 M NaCl/4% glucose, pH 7.4.

High-speed centrifugation: Almost the same way as that employed by Seaman *et al.* [27], the blood sample was fractionated within a period of 4–6 hrs by the high-speed centrifugation method of Murphy [29], using blood anti-coagulated with 1.5 mg $Na_2EDTA.2H_2O$/ml, and spun for 1 hr at 12,000 rpm at 25°C. The top 10% of the gradient was taken for harvesting young-Y-RBCs and the bottom 10% of the column was taken for harvesting old-RBCs.

Reagents

Analytical grade reagents were used. *SNA*-FITC (Vector Labs, Burlingame, CA, USA), positively charged CdSe/ZnS core-shell QDs (Wuhan Jiayuan QDs Company, Wu Han, China) were purchased. Suitable suspending medium and experimental conditions for QDs homogeneously dispersed in solution for labelling all the negative charges on cells were determined [30].

Fig. 1 The fluorescence of *SNA*-FITC bound to Y-RBCs and O-RBCs. (**A**) and (**B**), the fluorescence images, respectively, from *SNA*-FITC bound to Y-RBCs and O-RBCs which were fractionated by Percoll method. (**C**) The fluorescent intensities of Y-RBCs and O-RBCs fractionated, respectively, by Percoll and high-speed centrifugations determined by flow-cytometry. The error bars indicate the uncertainties of the measurements. The data were averaged from the results of the blood samples of 18 volunteers (10 males, 8 females). The t-tests indicate that there is a significant difference between the young cells and old cells in fluorescent intensities ($P < 0.001$) in the
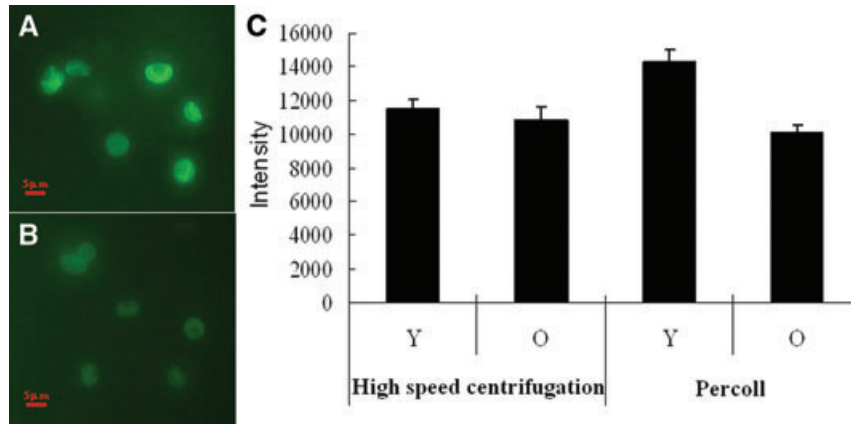
Percoll group, whereas there is no significant difference between the young cells and old cells ($P > 0.05$) in the high-speed centrifugation group.

Fluorescence microscopy

Fluorescence microscopy of cells labelled with the SA-specific *SNA*-FITC or QDs was done by an inverted fluorescence microscope (Nikon TE300; Nikon, Tokyo, Japan) with a digital camera (PCO, Kelheim, Germany). The exciting and emission wave lengths for the green *SNA*-FITC were: ~488 nm and 525 nm, respectively; for the QD-labelled RBCs, the exciting wavelength was centred at ~388 nm and emission wavelength was ~588 nm. To label the total surface charges of the RBCs, the QDs were dissolved in a 0.1 M phosphate-buffered saline solution (PH 7.4, at 37°C) with a concentration of 4.88 μmol/l. Then 1 μl of the QD solution was added to 200 μl of a buffer solution (5 ml 0.9% sodium chloride solution mixed with 10 ml of 5% glucose solution in the volume ratio of 1:2) with RBCs. The mixture was shaken gently, allowed to rest for at least 10 min. and then washed (×3) to get rid of unbound QDs. The method to label the RBCs with *SNA*-FITC is the same as reported previously [31].

Flow cytometry

Flow cytometry of Y-RBCs and O-RBCs labelled with the SA-specific *SNA*-FITC was done by a flow cytometer for the cells fractionated by Percoll and high-speed centrifugation. The exciting wavelength was 488 nm and emission wavelength was ~525 nm. Flow cytometry was also performed for the cells fractionated by Percoll to evaluate the sizes and densities of the Y-RBCs and O-RBCs by comparing the forward and sideward scattering.

ζ-potential measurements

A ζ PALS instrument (Brookhaven, New York, NY, USA) for phase-shift-based analysis light scattering [32] was used for determining ζ-potentials of cells suspended in 0.029 M NaCl/4% glucose ($5–8 \times 10^6$ cells/ml) (25°C), measuring ~1000 cells (triplicates for mean values). Each of the measurements was completed within 2,3s before electroendosmosis sets in, requiring no cuvette axis at right angle to the microscope axis alignment for ensuring measurements at the 'stationary level', where the electroendosmotic effect is zero (required for 'true' EPMs) [17–20]. Thus, the pres-

ent approach avoids/eliminates instrument related errors that is a great advantage.

Membrane deformability measurements

Measurement on the membrane deformability of RBC was performed by a typical micropipette aspiration technique and the membrane bending modulus K_c was determined by the technique of dynamic image analysis reported previously [31, 33].

## Raman spectroscopy of RBC Fractions in suspension

As described previously [34], the Raman spectra of living RBCs were recorded by a JY RAM INV system using 514.2 nm excitation line from an Ar^+ ion laser through an inverted Olympus optical microscope with a ×60 objective (Olympus, Tokyo, Japan). The acquisition band was 600–1800 cm^{-1} with a spectrum resolution of 1 cm^{-1}.

Raman spectra of young and old RBCs (prepared at 4°C) were recorded at different time intervals to discover any structural variation of the Hb and the T→R state transition speed of haemoglobin of RBC fractions. Additionally, line mapping was performed to study the distribution of Hb in single RBCs of different fractions. For detailed methods and procedure please see [34].

The Raman spectra of each group of RBCs were obtained by averaging the spectra measured from 25–30 cells of the group. The spectra of each cell in turn were averaged from the spectra measured at four to five random points on the cell. The signal-to-noise ratio (data not shown) in the measurement and the averaging show that the spectrum variations can be detected with an accuracy of about 2.8%.

Statistical analysis

The t-tests were performed for statistical analyses on the fluorescent intensities and ζ-potentials of different groups of cells using the SPSS 15.0 statistical software.
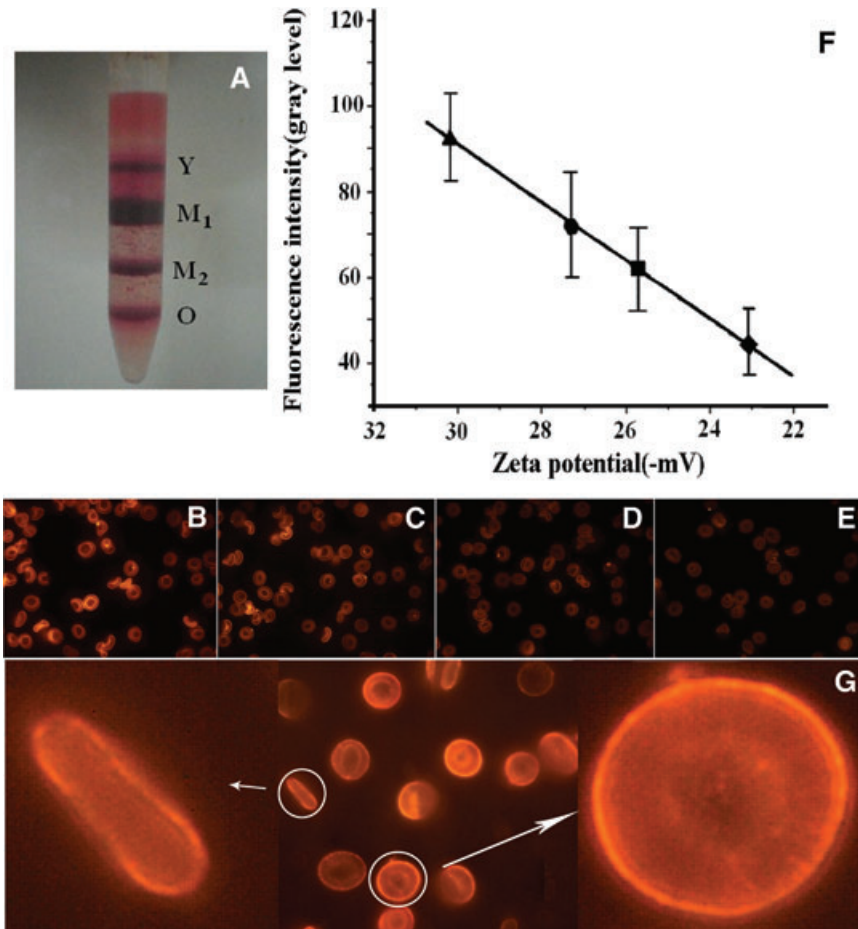
Fig. 2 RBCs fractionated by Percoll and the collinear relation between the fluorescent intensities and ζ-potentials of the cells in the fractions. (**A**) The four fractions of RBCs; their fluorescence images from QDs bound to Y-RBCs (**B**), M1 (**C**), M2 (**D**) and O-RBCs (**E**), respectively. (**F**) The collinear relation between the fluorescent intensities and ζ-potentials of the cells. (**G**) The enlarged images of QD-labelled Y-RBC. The error bars in (**F**) indicate the uncertainties of the measurements. The data were averaged from the results of the blood samples of 32 volunteers (20 males, 12 females). In ζ-potential measurement, each sample was measured four to five times. In QD fluorescent intensity measurements, each cell was measured at four to five random points; at least 50 cells were measured for each sample.

Table 1 Numbers of cells and ζ-potentials in the fractions harvested by the Percoll fractionation*

| Fraction	Cell numbers per ml (×10⁸)	ζ-potential (mV)
Lightest/top young	4.10 ± 0.21	−30.2 ± 1.2
Densest/bottom/old	1.73 ± 0.25	−23.2 ± 1.3
Middle fraction M1	1.56 ± 0.23	−27.5 ± 1.0
Middle fraction M2	3.60 ± 0.22	−25.7 ± 1.3

*Data were obtained from the measurements on the blood samples of 32 volunteers (20 males, 12 females). The t-tests using the SPSS 15.0 statistical software indicate that for the ζ-potentials; $P < 0.001$ for young RBCs *versus* old RBCs; $P < 0.01$ for young *versus* M1 RBCs, M1 *versus* M2, and M2 *versus* old RBCs.

Results

Figure 1 shows the fluorescence images from *SNA*-FITC bound to Y-RBCs and O-RBCs, which were fractionated by Percoll fraction-

ation. We can see that the fluorescence from Y-RBCs is much more intense than from O-RBCs. Figure 1C gives the fluorescent intensities of Y-RBCs and O-RBCs fractionated by Percoll and high-speed centrifugations determined by flow cytometry on thousands of cells. The images clearly indicate that the Y-RBCs fractionated by Percoll have much greater fluorescent intensity (or greater amount of SA) than O-RBCs, whereas the Y-RBCs and O-RBCs fractionated by high-speed centrifugation do not show any significant difference between the fluorescent intensities.

Figure 2A shows the adult human RBCs fractionated by Percoll: the lightest top fraction- young RBCs (denoted as Y), two middle fractions (M1 and M2) and the bottom, the densest fraction-old-RBCs (denoted as O). We can see that the four fractions were separated quite clearly. Figure 2B–E shows the fluorescence images from QD bound to Y-RBCs, M1, M2 and O-RBCs, which were fractionated by Percoll. We proved previously that by using the collinear relation between the fluorescent intensity and ζ-potential (or charge density), the fluorescent intensity at each pixel of the image can be used to estimate the magnitude of the surface charge density at the point [30]. Therefore, in Figure 2F the relation between the fluorescent intensities and the ζ-potentials for Y-RBCs,
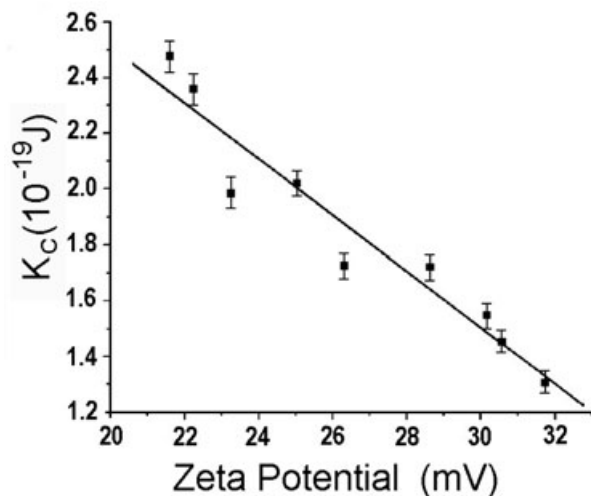
Fig. 3 The relationship between the membrane bending modulus K_c and the ζ-potential of aging RBCs. The error bars indicate the uncertainties of the measurements. They were averaged from the data measured on the blood samples of 32 volunteers (20 males, 12 females, at least 50 cells were measured for each sample).

M1, M2 and O-RBCs is shown to indicate that there is really a collinear relationship between the two parameters. Figure 2G presents the enlarged images of QD-labelled Y-RBC to clearly show that there is a very bright intense orange fluorescence ring around the cells and on the cell surface with the dark centre arising from the biconcave discoid doughnut shape of RBCs. Table 1 lists the detailed information about the numbers of cells and the averaged values of ζ-potential in each fraction harvested by the Percoll density centrifugation in 2 ml of peripheral blood from the well-defined layers. All these results show a gradual decrease of ζ-potentials of RBCs in the various fractions, *i.e.* from those in the lightest

fraction of Y-RBCs through to those in the middle fractions, M1, M2 down to the densest O-RBCs, revealing a collinear relationship between the decreasing ζ-potentials and the intensity of fluorescence from QDs bound to all the electron charges on the cell fractions. These differences between ζ-potentials were independent of gender.

The membrane bending modulus, K_c for Y-RBCs was found to be $1.48 \pm 0.17 (\times 10^{-19}$ J$)$ and increased to 2.19 ± 0.20 $(\times 10^{-19}$ J$)$ for O-RBCs. Because the deformability of a RBC is inversely proportional to K_c, it means that with RBC aging the unique deformability [31, 33, 34] is decreased. To see if there is also a collinear relationship between the membrane bending modulus K_c and the ζ-potentials of aging RBCs, we constructed a simulative curve for the relationship (Fig. 3). It clearly shows that K_c collinearly changes with ζ-potential [$Y = 4.51167 - 0.100115X$; $R = -0.96096$; $P < 0.001$].

In the capillary aspiration experiments, we measured the time for a cell to be drawn completely into the capillary (inner diameter 1.8 μm) under a constant suctioning pressure. The time for O-RBCs to get through the capillary under a negative pressure of 1500 pa was 0.87 sec., longer than the time for Y-RBCs (0.67 sec.), thus suggesting greater stiffness of O-RBCs. This simulates and parallels the situation of RBCs in circulation.

Old RBCs more often were found to be spherocytes, although echinocytes were also observed. The contact area ($27.5 \pm 2.16 \ \mu$m^2) and the major axes ($6.16 \pm 0.22 \ \mu$m) of aged cells were significantly smaller ($P < 0.05$) than those for Y-RBCs ($28.31 \pm 2.52 \ \mu$m^2 and $6.81 \pm 027 \ \mu$m, respectively). In O-RBC suspensions, cell aggregation was also observed. The flow cytometry measurements on huge numbers of RBCs shown in Figure 4 also indicate that the O-RBCs fractionated by Percoll have a greater density but are smaller in size than Y-RBCs.

Figure 5 shows the results of Raman spectroscopy of Hb in intact Y-RBCs and O-RBCs. As reported previously [35], O-RBCs have characteristic Raman bands similar to that for Y-RBCs but are more intense at the bands of 674, 850, 1359, 1587 and 1609 cm^{-1}

Fig. 4 The flow cytometry on the size and density of O-RBCs (left) and Y-RBCs (right).
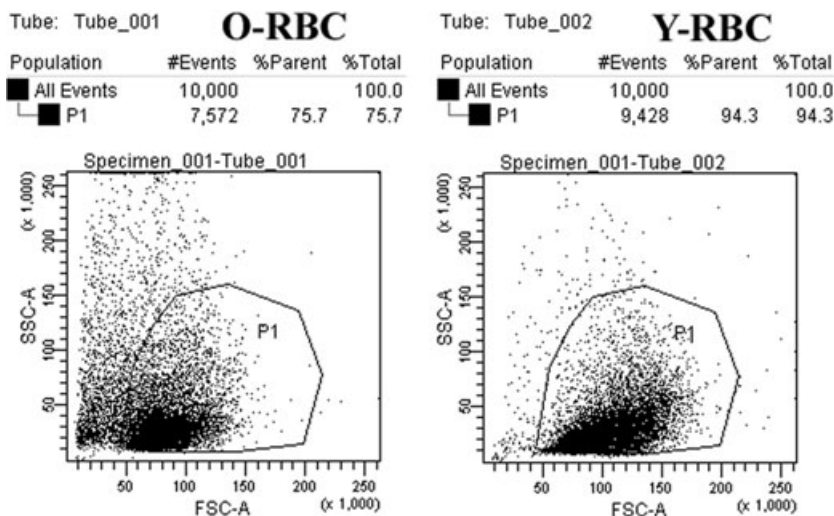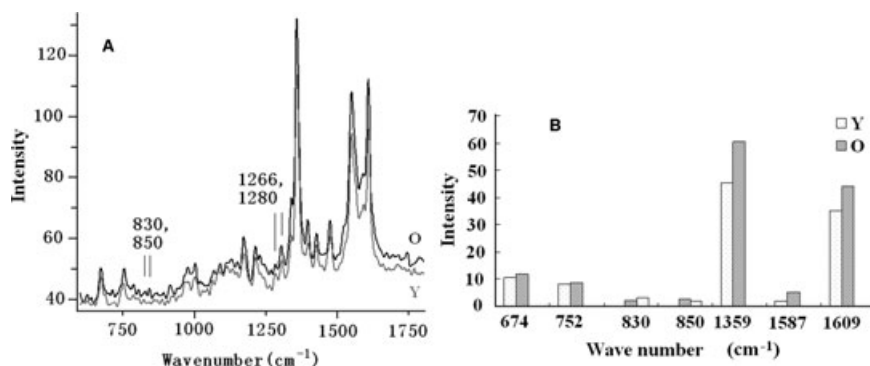
Fig. 5 The Raman spectroscopy of Hb in intact Y-RBCs and O-RBCs (**A**) and the peak intensities at different bands (**B**).

(Fig. 5B). The intensity ratio of I_{830}/I_{850} in O-RBC Raman spectra is <1 in contrast to >1 for Y-RBC. The concentration increment of the Hb in an old RBC is owing to its volume reduction. Whereas I_{830}/I_{850} < 1 suggests that tyrosine is exposed in the Hb of O-RBCs, and there appears to be some degree of aggregation and change/transformation in the side chains of its intracellular Hb. These observations thus indicate that the intracellular Hb in old RBC has some structural changes in the tyrosine residue and peptide chain of globin. There may also be some degree of denaturation, such as, the increase of unordered coil, in contrast to young RBCs.

A similar situation also happens for the time needed for the intracellular Hb to transit from deoxygenated taut/(T) state to oxygenated relaxed/(R) state in Y-RBCs and O-RBCs. The time-dependent oxygenation scores of Y-RBCs and O-RBCs show clear differences from after ~30 min., as found previously [35].

The Hb distribution in cells determined with line mappings and 2D mapping of the Raman signal at 1358 cm^{-1} band show that, in contrast to the homogeneous/uniform distribution of Hb in Y-RBCs, the protein intensity is much higher at the inner edges of O-RBC than in its centre. This indicates more Hb molecules distributed around the inside of cell membrane [35].

Discussion

The extensive robust data on ζ-potentials of vast numbers of RBCs from 38 donors blood confirm (*1*) the gradually decreasing ζ-potential (surface charge density, EPM) of RBCs with increasing densities; (*2*) ζ-potential of O-RBCs (−23.2 mV) was found decreased by ~30% compared to Y-RBCs (−30.2 mV) confirming perfect agreement with the 1961 data [24, 26]. This decrease of ζ-potential of O-RBCs by 7 mV equals 2.5×10^6 electron charges or 4×10^{-13} Coulomb per O-RBC. It is reassuring that substantially decreased charges on O-RBCs were confirmed by investigations on aliquots of cells by fluorescence imaging of Y,O-RBCs labelled with the SA-specific *SNA*-FITC as well as QDs (that label all the electron charges), O-RBCs showing significantly decreased fluorescence; (3) collinear relationship between the gradually decreasing ζ-potential of Y-RBCs to O-RBCs and the intensity of bright orange fluorescence from QDs bound to RBCs of various densities/ages. In view of the extensive data now presented using the modern technology, it is verified that in the aging of a RBC, its surface charge density/ζ-potential is decreased as SA is lost. Especially, the fluorescent images of Y and O-RBCs labelled with the SA-specific *SNA*-FITC and QDs, providing direct visual evidence of the amount of SA and charge density on the cells, clearly show significant differences in the SA and surface charge densities on Y-RBCs and O-RBCs. These pieces of evidence do not support the hypothesis by Seaman *et al.* [27] that the decrease of surface area in O-RBCs could compensate for the decrease of their surface SA, so that the surface charge densities as well as the EPMs of O-RBCs were observed to be similar to those of Y-RBCs. There are several possibilities for Seaman *et al.* not finding differences between the EPMs of their density centrifugation fractionated Y and O-RBCs that most likely arose from technical reasons and inadequate measurements [27, 28] on only 30 cells each from three to six donors. According to our results about the comparison between the ζ-potentials of the RBCs fractionated by Percoll and by high-speed centrifugation, at least one possible cause is clear. It relates to the fact, as pointed by many workers (see [2] and several other references therein), that neither high-speed centrifugation nor simple density centrifugation is able to achieve significant demarcation/separation clearly between Y- and O-RBCs (Fig. 2). Therefore, it was difficult for Seaman *et al.* [27, 28] to find differences between the EPMs of their 'Y' and 'O'-RBCs fractionated by high-speed centrifugation.

Extensive writings [2, 8, 9] are persuasive that the age-related changes in band-3, (4.1a, 4.1b ratio) [9], neoantigens and aggregated IgG on densest/senescent O-RBCs with bound autoantibodies, signal the resident macrophages they are tuned to recognize for elimination.

As is clear from Figure 3, we discovered a collinear decrease of membrane deformability. O-RBCs, presumably, with their impaired deformability becoming too stiff to negotiate narrow capillaries in the spleen get stuck and eliminated by the RES. For these steps of clearance of damaged/effete O-RBCs, we postulate physico-chemical factors important in these steps for clearance of damaged/effete RBCs as follows.

As stated, ζ-potentials govern cell interactions [17–19]. The high charge density (~10^7 electron charges/144 μm^2) [17–19] on RBCs normally keeps them apart from high-charge-bearing monocyte subsets [36–38] that give rise to equally highly charged subsets of macrophages.

Monocytes have an EPM of -0.95×10^{-8} m^2/(sv). During differentiation the negative surface charge density of monocytes/macrophages either changed or remained constant (ref. [39]: fig. 14.2). Under some experimental conditions the EPM -0.95×10^{-8} m^2/(sv) could increase to -1.09×10^{-8} m^2/(sv). Monocytes were known to reach a normal macrophage size of about 2000 μm^3) [39]. Macrophages of EPMs as high as -1.39×10^{-8} m^2/(sv) may well be present but in future will require confirmation.

Now, decreased cell surface charge is thought to favour (firmer) adhesion between surfaces [40, 41]. Two examples are that of decreased cell surface charge in the formation of firmer sheep RBC-lymphocyte rosettes after cells being treated with neauraminidase [42] and cystic fibrosis epithelia showing increased adherence of microorganisms known to cause chronic lung infection [43]. We suggest that senescent, O-RBCs bearing ~30% decreased ζ-potentials, *i.e.* weakened electrostatic barrier to be overcome by the awaiting monocytes/macrophages get closer, positioned for grabbing *via* the Fc-part for phagocytosis and clearance by the RES.

It has already been stated that the decrease of surface charge would lead to a collinear decrease of membrane deformability. As we suggested [31], the decrease of membrane deformability on one hand is due to the change of band 3 protein induced by the change in NANA carboxyls related charge, and on the other hand it results from the changes of the aggregation and distribution of the intracellular Hb. At physiological pH and ionic strength in an oxygen-linked fashion, Hb binds to the cytoplasmic domain of band 3 protein [44]. The predominant sites of binding for Hb on the inner surface of the red cell membrane are the two major integral membrane glycoproteins. For the Hb in an intact O-RBC, as revealed by our Raman spectroscopy data, the intracellular Hb structure is, presumably, disturbed so that its oxygenation is influenced. Some Hb molecules are aggregated and attach to the inside cell membrane (that presumably puts constraints on it). The binding of Hb to the inside cell membrane can not only lead to a reduction of the membrane flexibility [44], but also influences the oxygenation of Hb. It was suggested that when Hb is bound to the inside of the cell membrane, the reactive oxygen species generated in autoxidation are not efficiently neutralized by the cellular antioxidant enzymes [45, 46].

Concluding remarks

Flawed techniques and manipulation-introduced artefacts, undoubtedly serious liabilities, are guarantees of failure and misleading data. We need to discover the precise nature of the progressive changes that occur in the surface membrane

structures, physico-chemical-electrical, mechanical properties (unique deformability) and function of RBCs affecting microcirculation.

Improved technology and multiparameteric study on 38 donors' blood and thousands of fractionated cells showed ~30% decreased charge on aged RBCs in excellent agreement with the original reports [25, 26]. These studies finally remove the ambiguity and uncertainty [27, 28] from 1961–1978 onwards. Striking differences between the young–old RBCs are confirmed by several techniques and parameters: membrane bending moduli, imaging surface SA, all electron charges/charge density and intracellular Hb structures. To separate RBCs with different ages clearly, it is recommended to use the Percoll method for fractionation that is now generally considered appropriate and is used (see [2] and several other references therein).

The high quality of 'cleaned up' blood is of immense practical clinical importance worldwide. It is essential to set up simple routine monitoring quality control of blood in storage [1, 2] to avoid the serious adverse effects [3, 10–12] by pathophysiological biomaterials released from damaged cells accumulating and requiring removal. Tackling this is clearly urgent. A multidisciplinary approach is the most hopeful for continuing to develop reliable methods for blood storage and sound rational bases for reliable therapeutic programs as free from risk as possible.

Another contribution of the present investigation is that it reveals the close correlation between the surface charge of a RBC and its structure and functions, from the morphology of the cell, the membrane deformability to the intracellular Hb structure and oxidation ability.

Finally, we believe that our data are highly relevant to efficient oxygen delivery in health and disease and are likely to be of practical value in clinics. Separate experiments show that the deduced ζ-potentials from QDs fluorescence on labelled cells, were in perfect agreement with the values determined by ζ PALS instrument. QD-labelled cell imaging provides for the first time direct evidence of the difference between the surface charge densities of O- and Y-RBCs, and the ability of quantitative visual detection on total charge density of living cells. This unique combination of quantitative biophysical parameters (in terms of millivolts and fluorescence intensity levels) would be of practical value in routine automated monitoring of large numbers of samples in clinics and blood banks. Quality control using zetametry (and other similar methods) with QD/lectins imaging on snapshot samples (2 ml), would facilitate automated monitoring of large numbers of samples to achieve improved blood storage as free from risk as possible. It is understood of course that transfusion of stored blood after thoroughly testing for infections is as safe as it ever can and will be.

It is not overstating that our novel quantitative biophysical–electrical approach is likely to be of practical value in clinics before/during/after therapy, such as for haemorheologcal, circulatory disorders, abnormal red cells, macrophages (*e.g.* in Gaucher disease), respiratory physiology, hypoxia, mountaineers-Everest climbers, residents at high altitudes, neocytolysis in astronauts after space flights requiring treatment of anaemia, renal pathology,

erythropoietin doping in sports/athletes, improving blood storage and monitoring blood quality control.

Conflict of interest

The authors confirm that there are no conflicts of interest.

References

1. **Chin-Yee I, Arya N, d'Almeida M**. The red cell storage lesion and its implication for transfusion. *Transfus Sci.* 1997; 18: 447–58.
2. **Bosman GJ, Werre JM, Willekens FL, et al.** Erythrocyte ageing *in vivo* and *in vitro*: structural aspects and implications for transfusion. *Transfus Med.* 2008; 18: 335–47.
3. **Adamson JW**. New blood, old blood, or no blood? *N Engl J Med.* 2008; 358: 1295–6.
4. **Gladwin M, Shapiro K, Daniel B.** Storage lesion in banked blood due to hemolysis-dependent disruption of nitric oxide homeostasis. *Curr Opinion Hematol.* 2009; 16: 515–23.
5. **Klein H, Anstee D.** Mollison's blood transfusion in clinical medicine. 11th ed. Oxford: Oxford Blackwell; 2005.
6. **Mazor D, Dvilansky A, Meyerstein N**. Prolonged storage of red cells: the effect of pH, adenine and phosphate. *Vox Sang.* 1994; 66: 264–9.
7. **Hillyer C, Silberstein L, Ness P, et al.** Blood banking and transfusion medicine: basic principles & practice. Livingstone: Churchill; 2006.
8. **Lutz HU, Stringaro-Wipf G.** Senescent red cell-bound IgG is attached to band 3 protein. *Biomed Biochim Acta.* 1983; 42: S117–21.
9. **Lutz HU, Bussolino F, Flepp R, et al.** Naturally occurring anti-band 3 antibodies and complement together mediate phagocytosis of oxidatively stressed human erythrocytes. *Proc. Natl. Acad. Sci. USA.* 1987; 84: 7368–72.
10. **Murphy GJ, Reeves BC, Rogers CA, et al.** Increased mortality, postoperative morbidity, and cost after red blood cell transfusion in patients having cardiac surgery. *Circulation.* 2007; 116: 2544–52.
11. **Spinella P, Carroll C, Staff I, et al.** Effect of red blood cell storage is associated with increased incidence of deep vein thrombosis and in hospital mortality in patients with traumatic injuries. *Crit Care.* 2009; 13: R151 (1–11).
12. **Koch C, Li L, Sessler D, et al.** Duration of red-cell storage and complications after cardiac surgery. *N Engl J Med.* 2008; 358: 1229–39.
13. **Klenk E, Uhlenbruck G.** Über neuraminsauerehältgies Mucoide aus Menschenrerythrocytenstroma. [On the isolation of mucoids containing neuraminic acid from human erythrocyte stroma, a contribution to the chemistry of agglutinogens.] *Hoppe Seylers Z Physiol Chem.* 1960; 319: 151–60.
14. **Klenk E.** In: Wolstenholme GEW, O'Connor M, editors. The chemistry and biology of stone ucopolysaccharides. London: Ciba Foundation Symposium. J. & A. Churchill; 1958.
15. **Klenk E, Faillard H, Lempfrid H.** Über die enzymatische Wirkung von Influenzavirus (Enzymatic effect of the influenza virus). *Hoppe Seylers Z Physiol Chem.* 1955; 301: 235–46.
16. **Piper W.** Investigations of the effect of receptor destroying enzyme' on human erothrocytes. *Acta Haemat.* 1957; 18: 414–28.
17. **Abramson HA.** The cataphoretic velocity of mammalian red blood cells. *J Gen Physio.* 1929; 12: 711–25.
18. **Mehrishi JN.** Molecular aspects of the mammalian cell surface. *Prog Biophys Mol Biol.* 1972; 25: 1–70.
19. **Seaman GVF.** Electrokinetic behavior of red cells. In Surgenor, D. Mac N. editor. The red blood cell. 2nd ed. New York: Academic; 1975. p. 1135–229.
20. **Cook G, Heard D, Seaman G.** Sialic acids and the electrokinetic charge of human erythrocytes. *Nature.* 1961; 191: 44–7
21. **Eylar EH, Madoff MA, Brody OV, et al.** The contribution of sialic acid to the surface charge of the erythrocyte. *J Biol Chem.* 1962; 237: 1992–2000.
22. **Mehrishi JN, Bauer J.** Electrophoresis of cells and the biological relevance of surface charge. *Electrophoresis.* 2002; 23: 1984–94.
23. **Durocher JR, Payne RC, Conrad ME.** Role of sialic acid in erythrocyte survival. *Blood.* 1975; 45:11–20.
24. **Danon D, Marikovsky Y.** Différence de charge électrique de surface entre érythrocytes jeunes et âgés. [Difference of surface electric charge between young and old erythrocytes]. *Compte Rendu Acad Sci Biol D.* 1961; 253: 1271–2.
25. **Marikovsky Y, Danon D.** Electron microscope analysis of young and old red blood cells stained with colloidal iron for surface charge evaluation. *J Cell Biol.* 1969; 43: 1–7.
26. **Yaari A.** Mobility of human red blood cells of different age groups in an electric field. *Blood.* 1969; 33: 159–63.
27. **Seaman G, Knox R, Nordt F, et al.** Red cell aging. I. Surface charge density and sialic acid content of density-fractionated human erythrocytes. *Blood.* 1977; 50: 1001–11.
28. **Luner S, Szklarek D, Knox R, et al.** Red cell charge is not a function of cell age. *Nature.* 1977; 269: 719–21.
29. **Murphy G.** Influence of temperature and method of centrifugation on the separation of erythrocytes. *J Lab Clin Med.* 1973; 82: 334–41.
30. **Huang Y-X, Zheng X-J, Kang L-L, et al.** Quantum dots as a sensor for quantitative visualization of surface charges on single living cells with nano-scale resolution. *Biosens Bioelectron.* 2011; 26: 2114–8.
31. **Chen XY, Huang YX, Liu WJ, et al.** Membrane surface charge and morphological and mechanical properties of young and old erythrocytes. *Current Appl Phys.* 2007; 7: e94–6.

32. **Tscharnuter WW.** Mobility measurements by phase analysis. *Appl Opt.* 2001; 40: 3995–4003.

33. **Li J, Huang YX.** Superresolution measurement on the minute fluctuation of cell membrane. *Chin Sci Bull.* 2006; 51: 143–7.

34. **Kang LL, Huang YX, Liu WJ, et al.** Confocal Raman microscopy on single living young and old erythrocytes. *Biopolymers.* 2008; 89: 951–9.

35. **Musielak M.** Red blood cell-deformability measurement: review of techniques. *Clin Hemorheol Microcirc.* 2009; 42: 47–64.

36. **Passlick B, Flieger D, Ziegler-Heitbrock H.** Identification and characterization of a novel monocyte subpopulation in human peripheral blood. *Blood.* 1989; 74: 2527–34.

37. **Ziegler-Heitbrock H, Fingerle G, Strobel MWS, et al.** The novel subset of CD14+/CD16+ blood monocytes exhibits features of tissue macrophages. *Eur J Immunol.* 1993; 23: 2053–8.

38. **Varol C, Yona S, Jung S.** Origins and tissue-context-dependent fates of blood monocytes. *Immunol Cell Biol.* 2009; 87: 30–8.

39. **Bauer J.** Cell electrophoresis. Boca Raton, FL: CRC Press; 1994.

40. **Curtis ASG.** The cell surface – its molecular role in morphogenesis. London: Logos Press; 1967.

41. **Mege JL, Capo C, Benoliel A-M, et al.** Use of cell contour analysis to evaluate the affinity between macrophages and glutaraldehyde-treated erythrocytes. *Biophys J.* 1987; 52: 177–86.

42. **Hanjan SN, Talwar GP, Kidwai Z, et al.** Delineation and quantitation of human peripheral blood lymphocyte subpopulations by electrophoretic mobility and role of surface charge in cell to cell interaction. *J Immunol.* 1977; 118: 235–41.

43. **Bongrand P, Capo C, Mège J, et al.** Surface physics and cell adhesion. In: Bongrand P, editor. Physical basis of cell-cell adhesion. Boca Raton, FL: CRC Press; 1988. p. 91–123.

44. **Hiroshi I.** Effects of abnormal Hb on red cell membranes. *Jpn J Clin Pathol.* 1999; 47: 232–7.

45. **Rauenbuehler PB, Cordes KA, Salhany JM.** Identification of the hemoglobin binding sites on the inner surface of the erythrocytes membrane. *BBA.* 1982; 692: 361–70.

46. **Salhany JM, Cassoly R.** Kinetics of p-mercuribenzoate binding to sulfhydryl groups on the isolated cytoplasmic fragment of band 3 protein. Effect of hemoglobin binding on the conformation. *J Biol Chem.* 1989; 264: 1399–404.